


RESEARCH ARTICLE

Anatomical texture patterns identify cerebellar distinctions between essential tremor and Parkinson's disease

Kilian Hett¹  | Ilwoo Lyu¹ | Paula Trujillo² | Alexander M. Lopez² | Megan Aumann² | Kathleen E. Larson¹ | Peter Hedera^{2,3} | Benoit Dawant¹ | Bennett A. Landman¹ | Daniel O. Claassen² | Ipek Oguz¹

¹Department of Electrical Engineering and Computer Science, Vanderbilt University, Nashville, Tennessee

²Department of Neurology, Vanderbilt University Medical Center, Nashville, Tennessee

³Department of Neurology, University of Louisville, Louisville, Kentucky

Correspondence

Kilian Hett, Department of Electrical Engineering and Computer Science, Vanderbilt University, Nashville, TN.
Email: kilian.hett@vanderbilt.edu

Funding information

NIH Clinical Center, Grant/Award Numbers: R01- NS095291, R01-NS094456, R01-NS0997783, U01-NS106845; Vanderbilt Medical Scholars Program, Grant/Award Number: UL1 RR 024975; Vanderbilt University

Abstract

Voxel-based morphometry is an established technique to study focal structural brain differences in neurologic disease. More recently, texture-based analysis methods have enabled a pattern-based assessment of group differences, at the patch level rather than at the voxel level, allowing a more sensitive localization of structural differences between patient populations. In this study, we propose a texture-based approach to identify structural differences between the cerebellum of patients with Parkinson's disease ($n = 280$) and essential tremor ($n = 109$). We analyzed anatomical differences of the cerebellum among patients using two features: T1-weighted MRI intensity, and a texture-based similarity feature. Our results show anatomical differences between groups that are localized to the inferior part of the cerebellar cortex. Both the T1-weighted intensity and texture showed differences in lobules VIII and IX, vermis VIII and IX, and middle peduncle, but the texture analysis revealed additional differences in the dentate nucleus, lobules VI and VII, vermis VI and VII. This comparison emphasizes how T1-weighted intensity and texture-based methods can provide a complementary anatomical structure analysis. While texture-based similarity shows high sensitivity for gray matter differences, T1-weighted intensity shows sensitivity for the detection of white matter differences.

KEYWORDS

cerebellar analysis, essential tremors, Parkinson's disease, texture analysis

1 | INTRODUCTION

Magnetic resonance imaging (MRI) analysis methods can detect anatomical brain changes within clinical populations, often by comparing structural differences between groups. These methods assess brain structure using high-level features (e.g., volume, surface area, cortical thickness, and shape). Voxel-based morphometry (VBM) is commonly employed as a method that compares anatomical differences without

the need for prior knowledge of specific regions of interest (Ashburner & Friston, 2000). VBM is a statistical framework that assesses differences at the voxel level between two different patient populations and is commonly interpreted by assessing morphologic features (Price et al., 2004), such as T1-weighted intensity (Tong et al., 2016), tissue probability density (Mechelli et al., 2005), or features from other MRI modalities such as DTI coefficients (Maggipinto et al., 2017).

This is an open access article under the terms of the Creative Commons Attribution-NonCommercial License, which permits use, distribution and reproduction in any medium, provided the original work is properly cited and is not used for commercial purposes.

© 2021 The Authors. *Human Brain Mapping* published by Wiley Periodicals LLC.

In recent years, texture-based analysis, which models local patterns of relative intensity variations rather than the absolute value of intensity, has proven a useful neuroimaging tool. Texture-based analysis can detect group-level differences not evident at the voxel scale (Cai et al., 2020). Unlike a voxel-wise approach, the texture-based analysis aims to describe variations in the patterns of spatial intensity along with a specific orientation. Recently, we developed a texture-based similarity method (Hett et al., 2018), which applies a patch-based approach to model the textural pattern at each voxel. This method integrates image neighborhood information and offers an improved capability to detect subtle anatomical changes (Coupé et al., 2012; Hett et al., 2019; Hett et al., 2020; Hett et al., 2016). Specifically, each voxel is associated with a value representing the similarity of textural patterns to two different groups of subjects. This results in an additional descriptor similar to those commonly used by VBM, which can also provide complementary information (Ding et al., 2015).

This novel texture-based method was originally described for the examination of pathological changes in the hippocampus (Hett et al., 2018), and have been adapted in this study to investigate the structure of the cerebellum. The cerebellum has been understudied as a result of contrast and resolution limitations of conventional structural MRI methods. The cerebellum is a major subdivision of the hindbrain and presents a relatively consistent anatomical structure. It is separated into two main structures: the cerebellar cortex, which is largely gray matter, and the deep cerebellar nuclei, which includes the cerebellar peduncles (white matter), and dentate nucleus (gray matter). The cerebellum is commonly divided into several lobules and vermis, which have distinct functional properties. For example, imaging studies show correlated activation of the dentate nucleus and inferior lobules associated with strategic motor control responses (Küper et al., 2014), while lateral posterior regions have been associated with cognition (Schmahmann, 2010).

Recent studies emphasize distinct changes to cerebellar structures in Parkinson's disease (PD) and essential tremor (ET) populations (Lin et al., 2013; Lopez et al., 2020). Both disorders commonly present with tremor and progressive worsening of motor function. In PD, tremor usually occurs at rest and involves several other symptoms such as bradykinesia, rigidity, and balance disruptions. In contrast, in ET, tremor in action movement is the primary symptom, and bradykinesia, rigidity, and balance issues are not commonly seen. The difference in so-called "action" and "postural" tremors in ET and PD suggests related but different pathologic substrates (Baumann, 2012; Algarni & Fasano, 2018; Schwindt & Rezmovitz, 2017).

Given the functional properties of the cerebellum, we sought to assess structural differences between ET and PD in this study. We assessed structural features at both a region-wise and voxel-wise level using two methods: i) MRI intensity using a classical VBM framework, and ii) a texture-based similarity method. We hypothesized that these analyses would provide complimentary results allowing for an assessment of the methodologic tradeoffs, as well as extend previous analyses that employed cerebellar volumetric assessments (Lopez et al., 2020), and VBM comparisons (Lin et al., 2013). We further hypothesized that a texture-based approach would provide greater sensitivity to group differences since this approach may alleviate limitations of volumetric and

VBM studies. In summary, in this study we propose a novel analysis to localize cerebellar differences between PD and ET populations, using a feature that is potentially more sensitive to group differences compared to the one used by the classic VBM approach.

2 | MATERIALS AND METHODS

2.1 | Demographics

This analysis was performed on 389 participants diagnosed with either PD ($n = 280$) or ET ($n = 109$) according to the established criteria proposed in (Hughes et al., 1993; Deuschl et al., 2008). The MRI data for all patients were acquired under anesthesia during a standard-of-care protocol for stereotactic planning of deep brain stimulation (DBS) surgery at Vanderbilt University Medical Center between 2011 and 2018. Motor impairment was quantified using the United Parkinson's disease rating scale (UPDRS) (Goetz et al., 2008) for PD patients and Washington Heights-Inwood Genetic study (WHIGET) for ET patients (Louis et al., 1997). The demographics details of the cohorts used in this study are summarized in Table 1.

2.2 | Image acquisition

MRI data were acquired using a 3.0 T Philips Achieva whole body scanner (Philips Medical Systems, Best, The Netherlands) with body coil radiofrequency transmission and sensitivity-encoded 8-channel head coil reception. T1-weighted MRIs were acquired using a 3D turbo field echo sequence (TR/TE = 7.92/3.65 ms; spatial resolution = $1 \times 1 \times 1 \text{ mm}^3$). Patients have been sedated for the duration of the MRI as part of the DBS protocol.

2.3 | Preprocessing

All images were pre-processed using the following pipeline (Figure 1): The cerebellum was segmented into 28 regions using a graph-cut approach (Yang et al., 2016) following the delineation protocol proposed by Bogovic et al. (2013). Denoising was performed with a spatially adaptive nonlocal mean filter (Manjón et al., 2012), followed by N4 bias-field correction (Tustison et al., 2010). Then, the union of the segmentation masks across the entire dataset was used to crop the cerebellum for the subsequent analyses. The intensity was normalized using a z-score standardization within the cerebellar volume, and finally an affine registration to the MNI space was performed (Avants et al., 2011).

2.4 | Anatomical features

Figure 1 summarizes the processing pipeline that was used in this study. Anatomical differences in the cerebellum were assessed using

TABLE 1 Demographic and clinical data

	Parkinson's disease	Essential tremor	p value
Number of subjects	280	109	
Age at scan (years)	62.1 ± 8.4	66.1 ± 9.6	< .01 ^a
Sex (F/M)	97/183	59/50	< .01 ^a
UPDRS-III off	42.35 ± 11.98	–	–
WHIGET off	–	28.40 ± 9.19	–

^aKruskal–Wallis test.

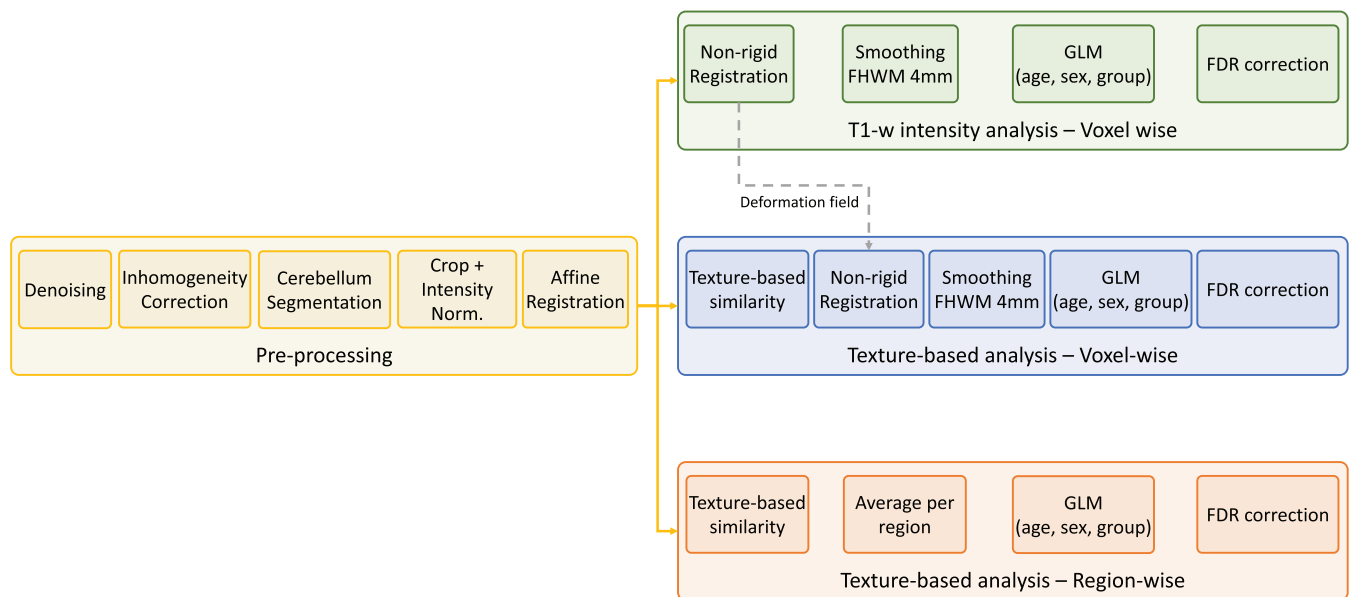


FIGURE 1 Processing pipeline. (Yellow) Common pre-processing steps applied on the input MRIs prior to all three analyses. (Green) Processing steps for the T1-w intensity analysis performed at the voxel level. (Blue) Processing steps for the texture-based similarity analysis performed at the voxel level. (Red) Processing steps for the texture-based similarity analysis performed at the region level

the T1-weighted intensity at a voxel scale, and a texture descriptor with two scales of analysis.

T1-weighted intensity: To achieve the voxel-wise comparison of T1-weighted intensity within the cerebellum, all MRIs were first aligned into the MNI ICBM-152 stereotaxic space (Fonov et al., 2011) using a nonrigid transformation (Avants et al., 2011). In order to reduce detection errors due to systematic misregistration and ensure that estimated features follow a normal distribution, T1-w images were spatially smoothed using a Gaussian filter with a FWHM (full width at half maximum) of 4 mm.

Texture-based similarity: The texture-based features were estimated using the patch-based grading approach proposed by Hett et al. (2018). This technique computes texture patterns within the entire cerebellar region for a given subject and compares this to two libraries of templates composed of patients suffering from PD and ET, respectively. To efficiently handle the complex shape of the cerebellum, the texture maps were computed along multiple directions using a bank of Gabor filters. A patch-based grading method was used to estimate the similarity of local patterns at each voxel using a patch size of 7 × 7 × 7 voxels. In our study, the libraries were constructed using an equal number of MRIs

from patients suffering from PD and ET (i.e., 60 patients from each group). In addition, to prevent any sex-related bias, the template libraries have been built with the same proportion of male and female patients. This texture-based method produces at each voxel a value between −1 (ET) to 1 (PD) representing the texture similarity (see Figure 2). Next, we computed two types of texture-based descriptor:

1. **Voxel-wise texture descriptor:** In order to make the texture-based features spatially comparable between subjects, we aligned all texture maps using a nonrigid transformation (Avants et al., 2011). The deformation fields were estimated using the T1-w MRI and the nonlinear MNI ICBM 152 template (Fonov et al., 2011).
2. **Region-wise texture descriptor:** Once the texture similarity has been estimated at each voxel, we used the lobule segmentation to aggregate these features within each cerebellar region. Relying on the lobule segmentation has two advantages. First, the subsequent anatomical descriptor is not dependent on the registration accuracy. Second, the average of texture within a given region provides a more robust anatomical descriptor than the relatively noisy voxel-wise descriptor.

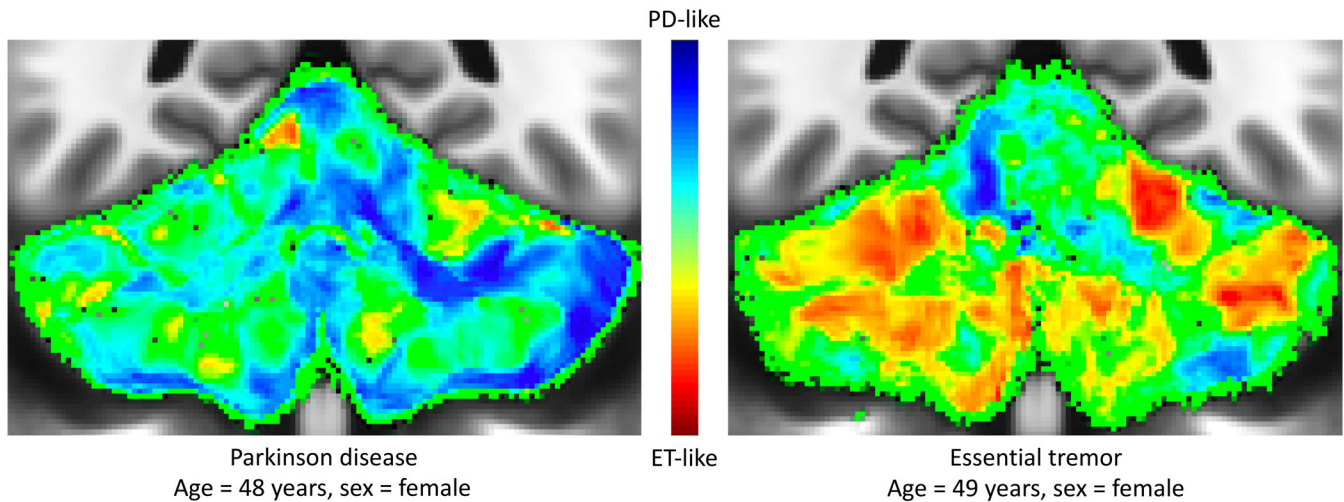


FIGURE 2 Example of two texture-based similarity maps after nonrigid registration to the MNI template. On the left side, a patient suffering from Parkinson's disease and on the right an age- and gender-matched patient suffering from essential tremor

2.5 | Statistical analysis

Because of the potential bias that age and sex can introduce, we used a similar statistical framework as employed in usual voxel-based morphometry methods to model the demographic effects and detect group differences. Consequently, once the T1-w images and texture-based similarity maps were estimated and aligned, we conducted a statistical analysis to localize areas with significant structural differences between PD and ET groups. To detect significant cerebellar differences, we used a general linear regression model (GLM) with the investigated anatomical features as dependent variables (i.e., T1-weighted intensity, voxel-wise texture, and region-wise texture descriptors), and patient pathologies, age and sex as co-variables. Finally, to control the false discovery rate (FDR) due to the large number of comparisons, p -values computed at each voxel were FDR-adjusted with the discovery rate q set to .05 using the method presented in (Benjamini & Hochberg, 1995). All p -values shown in the results have been FDR-adjusted. Analysis has been conducted within a bootstrapping scheme with 15 iterations. Bonferroni method was used to combine p -value maps obtained at each iteration. All statistical analyses have been conducted using MATLAB.

3 | RESULTS

3.1 | Intensity-based analysis

Figure 3 presents the spatial distribution of voxels with significant anatomical differences between PD and ET populations using T1-w intensities as features. In this figure, voxels with a negative regression coefficient (i.e., T1-w intensity smaller in ET patients than in PD patients) are displayed in blue and voxels with a positive coefficient (i.e., T1-w intensity larger in ET patients than in PD patients) are displayed in red. The results of our experiment suggest a lower intensity

for patients suffering from PD compared to ET population (shown in red), mostly located in the lobules and vermis VIII and IX. Significant differences were also found in the middle peduncle (corpus medullar). Any differences in the other regions did not reach statistical significance (see Figure 5c).

3.2 | Texture-based analysis

Voxel-wise analysis: Figure 4 presents the spatial distribution of discriminant texture-based features related to pathological differences in the cerebellum. We observe that the changes are symmetric in the inferior part of the cerebellar cortex and mostly right sided for the upper part of the cerebellum. Indeed, the discriminant texture features are primarily in the right lobules VI, VIIIa, VIIIb, and IX. All these lobules have a median p -value $< .05$ for the entire region (see Figure 4d). This indicates a highly localized texture difference. In addition, our experiments have also shown discriminant texture-based features in vermis Crus I/Crus II/VIIIb. Our experiments also indicate that lateral cerebellar lobules, such as VI, VII, VIII, and IX which border the vermis seem to present stronger structural differences between PD and ET. These findings are almost exclusively located in the gray matter. Significant texture-based differences were also found in corpus medullar, and specifically in the dentate nucleus area (see Section A of supplementary materials). For this comparison, the dentate nucleus was localized using the probabilistic atlas proposed in (He et al., 2017).

Region-wise analysis: Finally, we performed a regional texture-based analysis. The texture-based features have been averaged within each corresponding cerebellar area that have been identified using the segmentation method (Yang et al., 2016); which has recently shown to be comparable with state-of-the-art deep learning cerebellum parcellation methods (Han et al., 2020; Han et al., 2019). The Figure 4-B shows global texture differences for each cerebellar area. This

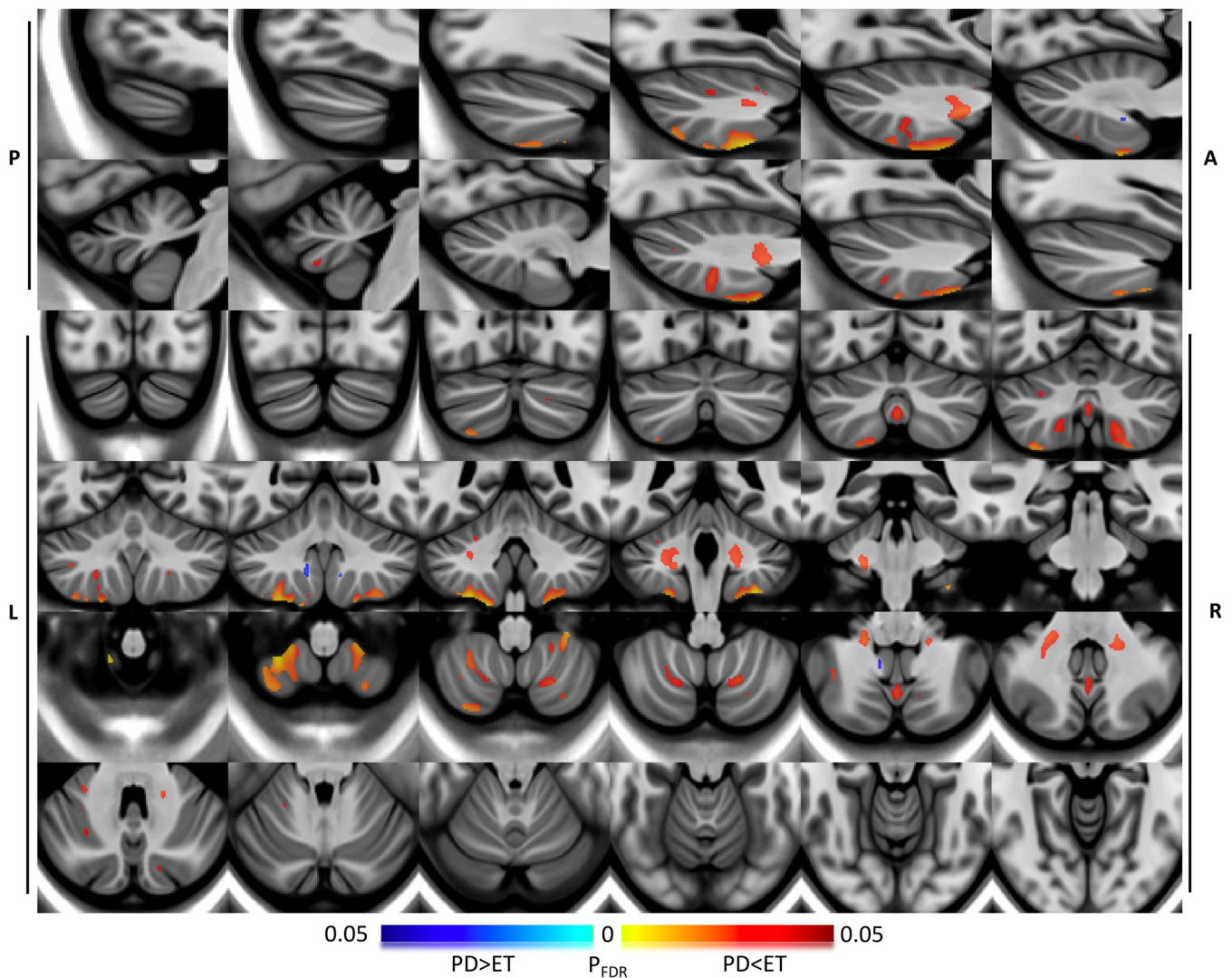


FIGURE 3 Voxel-wise T1w intensity analysis. Sagittal (top two rows), coronal (middle two rows) and axial (bottom two rows) views display the average of T1-w MRI over the entire considered cohort, with the spatial distribution of regression coefficients for voxels with discriminant intensity difference in color overlay. The p -value maps correspond to the diagnosis effect. p -values were adjusted using FDR-correction with a discovery rate set to $q = .05$. Only coefficients with p values inferior to $.05$ are displayed

experiment shows similar results to the voxel-wise analysis described above. Indeed, significant differences of region-wise texture-based similarity of PD and ET appear in lobule left Crus I (p -value = $.001$), vermis Crus I/Crus II/VIIIb (p -value = $.003$), lobules and vermis VIII (p -value < $.001$), and finally in lobules and vermis IX (p -values < $.001$).

4 | DISCUSSION

4.1 | Comparison of the T1-w intensity and texture features

In this study, we used two methods to assess the anatomical differences between patients with PD and ET. We evaluated the anatomical differences from T1-weighted intensities using a conventional VBM approach. This statistical framework enabled us to detect some

cerebellar structural differences between the two clinical cohorts, but has several limitations. Specifically, this method relies upon a series of preprocessing steps (i.e., interpolation and smoothing) that may have a negative impact on the results, obscuring subtle anatomical changes. In addition, it is well known that highly accurate registration tends to reduce signal differences between groups of patients. Therefore, to obtain robust results, VBM methods require a satisfactory tradeoff between good registration accuracy and the preservation of structural differences. Such compromise is by nature complicated to achieve and highly user-dependent. To overcome some of these limitations, we proposed to further evaluate anatomical differences using a recent texture-based similarity method (Hett et al., 2018). Contrary to VBM, texture-based similarities utilize only an affine transformation to help the detection of similar patches of texture. This results in preserving subtle anatomical information, which could provide better sensitivity to detect anatomical differences between patient populations.

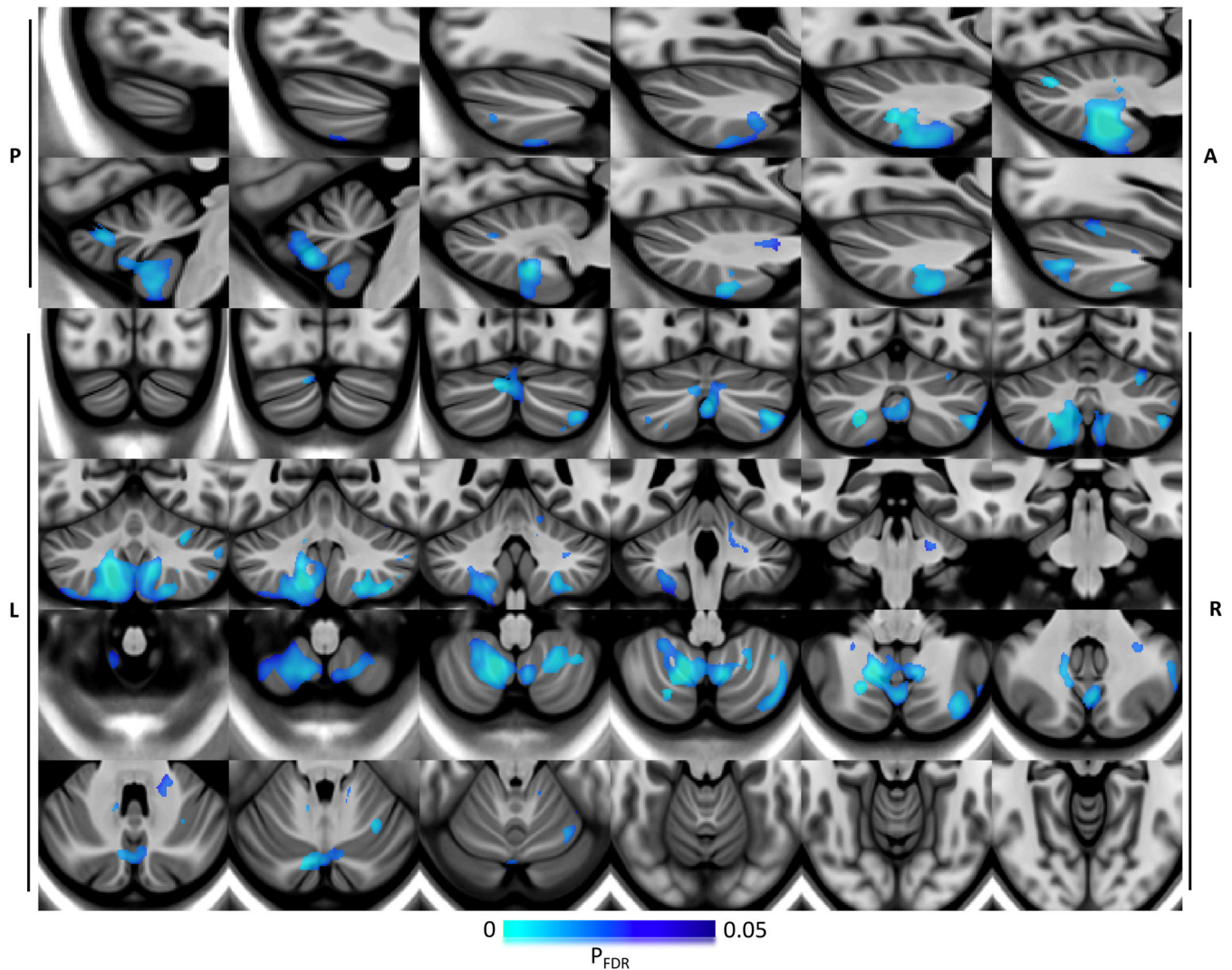


FIGURE 4 Voxel-wise texture similarity analysis. Sagittal (top two rows), coronal (middle two rows) and axial (bottom two rows) views showing the average of T1-w MRI over the entire considered cohort with the spatial distribution of voxels with discriminant texture differences in overlay. The p -value maps correspond to the diagnosis effect. p -values were adjusted using FDR-correction with a discovery rate set to $q = .05$. Only p -values inferior to .05 are displayed. We note that the values shown in this figure indicate group differences but do not represent a directional relationship (unlike Figure 3). This is because we analyze the texture similarity feature which estimates specific labels +1 and -1 for the PD and ET groups respectively, rather than analyzing the raw texture features directly

However, texture-based analysis is not without potential limitations. First, texture analysis tends to have reduced sensitivity in regions with low spatial variability such as the white matter. Moreover, the use of a patch for detecting anatomical differences also decreases precision in terms of spatial localization. This results in a potentially larger area detected compared to classic voxel-based morphometry. Another potential issue stems from the application of a denoising method before the texture analysis. We acknowledge that such preprocessing steps also tend to reduce high-frequency signals in the image which removes some of the subtle texture information. However, it has been shown that the SANLM method applied in our study enables us to preserve most of the texture information (Manjón et al., 2012).

In terms of the localization of the anatomical differences between the two groups, our results show that the T1-weighted intensity differences are mainly located in two distinct areas. First, we find group

differences in the cerebellar cortex in the left lobules VIIIb, VIII, vermis IX. Second, we find significant T1-weighted intensity differences in the corpus. The voxels with significant differences are mostly located in the middle peduncle, which is a white matter structure. Similar to the T1-weighted intensity analysis, the texture-based similarity analysis captures significant group differences mostly in the inferior part of the cerebellar cortex. The texture-based analysis revealed significant differences mainly located to the vermis crus I/crus II/VIIIb, vermis and lobules VIII, and IX. Moreover, the texture-based analysis also shows significant group differences in the left superior region of the cerebellar cortex (lobule VI), and the corpus, in the region of the dentate nucleus. In contrast, T1-w intensity analysis is inconclusive in the dentate (see Section A of supplementary materials). These findings are summarized in Figure 5 and in the supplementary materials (see Section B of supplementary materials).

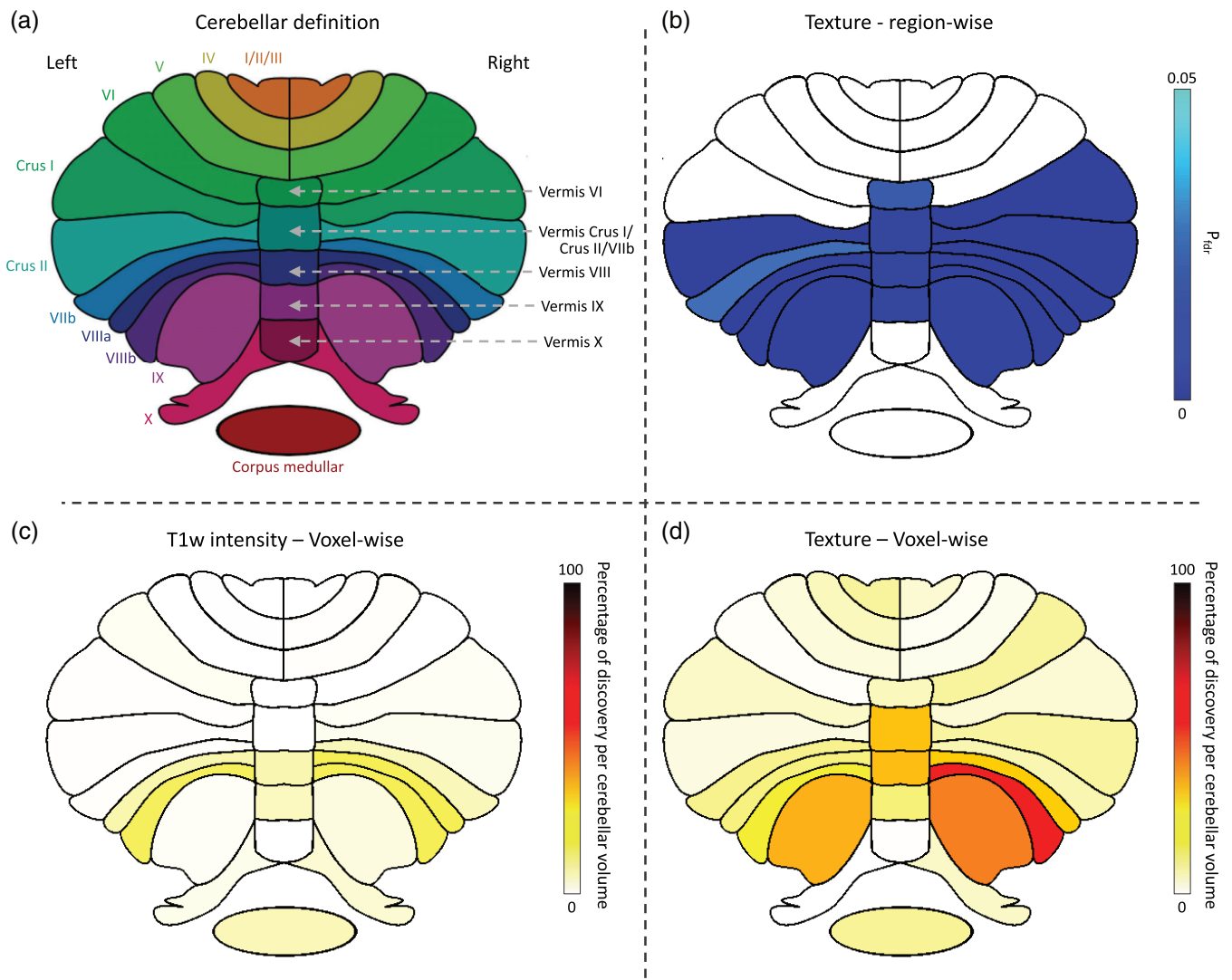


FIGURE 5 (a) Illustration of the segmentation protocol used in our study. (b) p -values obtained from the region-wise analysis of the texture descriptors after FDR correction. (c, d) Percentage of discovery per cerebellar region (estimated as the ratio of the number of voxels having significant differences over the volume of each corresponding region) for T1-weighted intensity and texture, respectively

Moreover, given the age difference between the two cohorts used in this study, we controlled for age in our analysis. Since the texture-based analysis relies upon template libraries, we incorporated an age matching technique to ensure a comparison between patients at similar ages. Age at the time of imaging was added as a covariate in the linear model.

4.2 | Physiopathology

Our study highlights regional cerebellar differences between PD and ET populations. First, it is interesting to note that differences in the vermis can explain symptomatic differences since it has been shown that such structures mediate gait and balance (Baumann, 2012; Stoodley et al., 2012). Secondly, the differences found in lobules VI

and VIII are in line with studies indicating that these lobules perform sensorimotor functions in the cerebellum (Lopez et al., 2020; Lewis et al., 2007; Sharifi et al., 2014; Benninger et al., 2009).

In addition to localized structural differences in the cerebellar cortex, our study showed two interesting findings located in the corpus medullar. Our results indicate anatomical differences in the middle peduncle. This might suggest differences between the modification of the cerebellum-thalamus-cortical circuit with the pathogenesis of PD and ET (Juttukonda et al., 2019). The analysis of the cerebellar texture also reveals anatomical pattern differences in the dentate nucleus, which is the largest structure that interfaces the cerebellar cortex to the rest of the brain (Sultan et al., 2010). It is interesting to note that even though the current image resolution does not enable us to clearly delineate this structure, the use of texture-based techniques might be sensitive enough to detect the structural differences of the

dentate nucleus. We hypothesize that the findings in the lobule VIII-IX and the dentate nucleus are likely explained by the correlation of activation associated with motor control responses in these two structures (Küper et al., 2014).

4.3 | Integrating previous literature

Motor involvements: Few neuroimaging studies have investigated the anatomical changes that occur in the cerebellum in the course of PD and ET. Among them, a VBM approach has compared cerebellar gray matter density differences between ET and a control population (Quattrone et al., 2008). This study revealed vermian atrophy which is more pronounced in ET patients with head tremor, but did not find anatomical differences for patients suffering from other types of tremors. A recent volumetric study evaluated the relationship of sensorimotor function and cerebellar atrophy (Lopez et al., 2020). This study identified group differences between PD and ET in the corpus medullar, lobule VI, lobules VIII. It is noteworthy that our findings are in line with these two studies. Moreover, the conducted texture-based analysis enables us to localize the anatomical differences in the corpus medullar and dentate nucleus in a more precise fashion than the volumetric analysis.

In addition to these two studies aiming to directly compare PD and ET cohorts to each other, several studies conducted separated comparison of PD and ET populations with control cohorts. A volumetric analysis indicated that only patients suffering from head tremors have cerebellar volume reduction (Cerasa et al., 2009). Another VBM approach studied cerebellar gray matter and white matter density to detect anatomical differences between ET and control population. This study did not find a group effect but indicated a correlation between gray matter density and the severity of intention tremor (Daniels et al., 2006). Finally, a VBM analysis examining gray matter density differences between PD patients and controls found that patients with resting tremors show decreased gray matter density in the posterior part of the quadrangular lobe compared to controls (Benninger et al., 2009). These latter findings are also consistent with the results of our study. We note that, since the PD and ET cohorts in our study were evaluated with different motor tests, our ability to link the MRI differences to motor phenotype is limited.

Nonmotor involvements: Also, because of the unbalanced sex proportion of the two cohorts in our study, we compared our findings with studies that analyzed the sex differences in the cerebellum among healthy participants. Previous literature shows mixed results, some studies suggest that sex differences are influenced in neural development, total size, but are negligible when accounting for total intracranial volume (Tiemeier et al., 2010; Raz et al., 2001). These studies suggest that the posterior lobe of the cerebellum accounts for the largest sex difference. Another study has also compared the anatomical differences of sex in the course of normal aging, but there were only significant in the vermis, and when participants are over the age of 70 years old (Oguro et al., 1998). Taking these results into account, and the fact that we co-varied for sex in all our analyses, we believe any imbalance in sex is unlikely to have influenced our results.

Finally, the cerebellum has been implicated in behavioral and psychiatric symptoms (Strick et al., 2009). A recent study using functional imaging indicated reduced coupling between lobule VI and VIIA-B with prefrontal, posterior parietal, and limbic regions, and an increased volume in lobule IX associated with major depression disorder (Depping et al., 2018). Another study highlights a degree centrality abnormality in the lobule VI for patients suffering from PD with depression (Wang et al., 2018). These confirm the findings of a previous study that suggested cerebellum changes in a PD population with depression (Ma et al., 2018). These studies emphasize the need to investigate cerebellar differences of nonmotor disturbances in neurodegeneration.

In summary, the texture-based method enabled us to capture subtle anatomical differences appearing in the cerebellum between PD and ET. We note significant differences between PD and ET populations in terms of cerebellar gray matter tissues in the lobules VII, VIII, and IX, and white matter differences in the corpus located in the dentate nucleus and middle peduncle.

4.4 | Strengths and limitations

In the proposed study we assessed anatomical texture to explore distinctions between persons with PD and ET. While the advanced method used in our analysis shows higher sensitivity for the detection of anatomical differences, we acknowledge that the present study has limitations in regards to the study population. Here, we consider the difference between two pathological cohorts without the comparison to a control group. Since the dataset is from patients undergoing DBS surgery, it does not include healthy controls. As a consequence, we are limited in interpreting the directionality of differences as compared to healthy controls. Therefore, future investigation is required to confirm the directionality of such differences.

ACKNOWLEDGMENTS

This work was supported, in part, by the NIH grants R01-NS094456, R01-NS0997783, R01-NS095291, and Vanderbilt Medical Scholars Program UL1 RR 024975. Vanderbilt University Institutional Review Board has approved this study.

DATA AVAILABILITY STATEMENT

The data that support the findings of this study are available on request from the corresponding author. The data are not publicly available due to privacy or ethical restrictions.

ORCID

Kilian Hett  <https://orcid.org/0000-0001-8831-4247>

REFERENCES

- Algarni, M., & Fasano, A. (2018). The overlap between essential tremor and Parkinson disease. *Parkinsonism & Related Disorders*, 46, S101–S104.
- Ashburner, J., & Friston, K. J. (2000). Voxel-based morphometry - the methods. *Neuroimage*, 11(6), 805–821.

- Avants, B. B., Tustison, N. J., Song, G., Cook, P. A., Klein, A., & Gee, J. C. (2011). A reproducible evaluation of ANTs similarity metric performance in brain image registration. *NeuroImage*, *54*(3), 2033–2044.
- Baumann, C. R. (2012). Epidemiology, diagnosis and differential diagnosis in Parkinson's disease tremor. *Park. Relat. Disord.*, *18*(SUPPL. 1), S90–S92.
- Benjamini, Y., & Hochberg, Y. (1995). Controlling the false discovery rate: A practical and powerful approach to multiple testing. *Journal of the Royal Statistical Society, Series B*, *57*(1), 289–300.
- Benninger, D. H., Thees, S., Kollias, S. S., Bassetti, C. L., & Waldvogel, D. (2009). Morphological differences in Parkinson's disease with and without rest tremor. *Journal of Neurology*, *256*(2), 256–263.
- Bogovic, J. A., Jedynak, B., Rigg, R., du, A., Landman, B. A., Prince, J. L., & Ying, S. H. (2013). Approaching expert results using a hierarchical cerebellum parcellation protocol for multiple inexpert human raters. *NeuroImage*, *64*(1), 616–629.
- Cai, J. H., He, Y., Zhong, X. L., Lei, H., Wang, F., Luo, G. H., ... Liu, J. C. (2020). Magnetic resonance texture analysis in Alzheimer's disease. *Academic Radiology*, *27*, 1774–1783.
- Cerasa, A., Messina, D., Nicoletti, G., Novellino, F., Lanza, P., Condino, F., ... Quattrone, A. (2009). Cerebellar atrophy in essential tremor using an automated segmentation method. *American Journal of Neuroradiology*, *30*(6), 1240–1243.
- Coupé, P., Eskildsen, S. F., Manjón, J. V., Fonov, V. S., Pruessner, J. C., Allard, M., ... Alzheimer's Disease Neuroimaging Initiative. (2012). Scoring by nonlocal image patch estimator for early detection of Alzheimer's disease. *NeuroImage: Clinical*, *1*(1), 141–152.
- Daniels, C., Peller, M., Wolff, S., Alfke, K., Witt, K., Gaser, C., ... Deuschl, G. (2006). Voxel-based morphometry shows no decreases in cerebellar gray matter volume in essential tremor. *Neurology*, *67*(8), 1452–1456.
- Depping, M. S., Schmitgen, M. M., Kubera, K. M., & Wolf, R. C. (2018). Cerebellar contributions to major depression. *Frontiers in Psychiatry*, *9*, 634.
- Deuschl, G., Bain, P., & Brin, M. (2008). Consensus statement of the Movement Disorder Society on tremor. *Movement Disorders*, *13*(S3), 2–23.
- Ding, Y., Zhang, C., Lan, T., Qin, Z., Zhang, X., & Wang, W. (2015). Classification of Alzheimer's disease based on the combination of morphometric feature and texture feature. In *Proceedings of IEEE international conference on bioinformatics and biomedicine, BIBM* (pp. 409–412). Washington, D.C. IEEE. <https://doi.org/10.1109/BIBM.2015.7359716>.
- Fonov, V., Evans, A. C., Botteron, K., Almli, C. R., McKinstry, R. C., & Collins, D. L. (2011). Unbiased average age-appropriate atlases for pediatric studies. *NeuroImage*, *54*(1), 313–327.
- Goetz, C. G., Tilley, B. C., Shaftman, S. R., Stebbins, G. T., Fahn, S., Martinez-Martin, P., ... Movement Disorder Society UPDRS Revision Task Force. (2008). Movement Disorder Society-sponsored revision of the unified Parkinson's disease rating scale (MDS-UPDRS): Scale presentation and clinimetric testing results. *Movement Disorders*, *23*(15), 2129–2170.
- Han, S., Carass, A., He, Y., & Prince, J. L. (2020). Automatic cerebellum anatomical parcellation using U-net with locally constrained optimization. *NeuroImage*, *218*, 116819.
- Han, S., He, Y., Carass, A., Ying, S. H., & Prince, J. L. (2019). Cerebellum parcellation with convolutional neural networks. *Medical Imaging: Image Processing*, 10949, 19.
- He, N., Langley, J., Huddleston, D. E., Ling, H., Xu, H., Liu, C., ... Hu, X. P. (2017). Improved neuroimaging atlas of the dentate nucleus. *Cerebellum*, *16*(5–6), 951–956.
- Hett, K., Ta, V.-T., Giraud, R., Mondino, M., Manjón, J. V., and Coupé, P. (2016). Patch-based DTI grading: Application to Alzheimer's disease classification. In Wu G., Coupé P., Zhan Y., Munsell B., Rueckert D. (eds), *Patch-Based Techniques in Medical Imaging. Patch-MI 2016*, Lecture Notes in Computer Science, 9993. New York, NY: Springer. https://link.springer.com/chapter/10.1007/978-3-319-47118-1_10.
- Hett, K., Ta, V. T., Manjón, J. V., & Coupé, P. (2018). Adaptive fusion of texture-based grading for Alzheimer's disease classification. *Computerized Medical Imaging and Graphics*, *70*, 8–16.
- Hett, K., Ta, V.-T., Oguz, I., Manjón, J. V., & Coupé, P. (2020). Multi-scale graph-based grading for Alzheimer's disease prediction. *Medical Image Analysis*, *67*, 101850.
- Hett, K., Ta V.-T., Catheline, G., Tournias, T., Manjón, J. V., Coupé, P. (2019). Multimodal hippocampal subfield grading for alzheimer's disease classification. *Scientific Reports*, *9*(1), <http://dx.doi.org/10.1038/s41598-019-49970-9>.
- Hughes, A. J., Lees, A. J., Daniel, S. E., & Blankson, S. (1993). A Clinicopathologic study of 100 cases of Parkinson's disease. *Archives of Neurology*, *50*(2), 140–148.
- Juttukonda, M. R., Franco, G., Englot, D. J., Lin, Y. C., Petersen, K. J., Trujillo, P., ... Claassen, D. O. (2019). White matter differences between essential tremor and Parkinson disease. *Neurology*, *92*(1), E30–E39.
- Küper, M., Wünnemann, M. J. S., Thürling, M., Stefanescu, R. M., Maderwald, S., Elles, H. G., ... Timmann, D. (2014). Activation of the cerebellar cortex and the dentate nucleus in a prism adaptation fMRI study. *Human Brain Mapping*, *35*(4), 1574–1586.
- Lewis, M. M., Slagle, C. G., Smith, A. B., Truong, Y., Bai, P., McKeown, M. J., ... Huang, X. (2007). Task specific influences of Parkinson's disease on the striato-thalamo-cortical and cerebello-thalamo-cortical motor circuitries. *Neuroscience*, *147*(1), 224–235.
- Lin, C.-H., Chen, C.-M., Lu, M.-K., Tsai, C.-H., Chiou, J.-C., Liao, J.-R., & Duann, J.-R. (2013). VBM reveals brain volume differences between parkinson's disease and essential tremor patients. *Frontiers in Human Neuroscience*, *7*. <http://dx.doi.org/10.3389/fnhum.2013.00247>.
- Lopez, A. M., Trujillo, P., Hernandez, A. B., Lin, Y.-C., Kang, H., Landman, B. A., ... Claassen, D. O. (2020). Structural correlates of the sensorimotor cerebellum in parkinson's disease and essential tremor. *Movement Disorders*, *35*(7), 1181–1188. <http://dx.doi.org/10.1002/mds.28044>.
- Louis, E. D., Ottman, R., Ford, B., Pullman, S., Martinez, M., Fahn, S., & Hauser, W. A. (1997). The Washington Heights-Inwood genetic study of essential tremor: Methodologic issues in essential-tremor research. *Neuroepidemiology*, *16*(3), 124–133.
- Ma, X., Su, W., Li, S., Li, C., Wang, R., Chen, M., & Chen, H. (2018). Cerebellar atrophy in different subtypes of Parkinson's disease. *Journal of the Neurological Sciences*, *392*, 105–112.
- Maggipinto, T., Bellotti, R., Amoroso, N., Diacono, D., Donvito, G., Lella, E., ... Alzheimer's Disease Neuroimaging Initiative. (2017). DTI measurements for Alzheimer's classification. *Physics in Medicine and Biology*, *62*(6), 2361–2375.
- Manjón, J. V., Coupé, P., Buades, A., Louis Collins, D., & Robles, M. (2012). New methods for MRI denoising based on sparseness and self-similarity. *Medical Image Analysis*, *16*(1), 18–27.
- Mechelli, A., Price, C., Friston, K., & Ashburner, J. (2005). Voxel-based morphometry of the human brain: Methods and applications. *Current Medical Imaging Reviews*, *1*(2), 105–113.
- Oguro, H., Okada, K., Yamaguchi, S., & Kobayashi, S. (1998). Sex differences in morphology of the brain stem and cerebellum with normal ageing. *Neuroradiology*, *40*(12), 788–792.
- Price, S., Paviour, D., Scahill, R., Stevens, J., Rossor, M., Lees, A., & Fox, N. (2004). Voxel-based morphometry detects patterns of atrophy that help differentiate progressive supranuclear palsy and Parkinson's disease. *NeuroImage*, *23*(2), 663–669.
- Quattrone, A., Cerasa, A., Messina, D., Nicoletti, G., Hagberg, G. E., Lemieux, L., ... Salzone, M. (2008). Essential head tremor is associated with cerebellar vermis atrophy: A volumetric and voxel-based morphometry MR imaging study. *American Journal of Neuroradiology*, *29*(9), 1692–1697.
- Raz, N., Gunning-Dixon, F., Head, D., Williamson, A., & Acker, J. D. (2001). Age and sex differences in the cerebellum and the ventral pons: A

- prospective MR study of healthy adults. *American Journal of Neuroradiology*, 22(6), 1161–1167.
- Schmahmann, J. D. (2010). The role of the cerebellum in cognition and emotion: Personal reflections since 1982 on the dysmetria of thought hypothesis, and its historical evolution from theory to therapy. *Neuropsychology Review*, 20(3), 236–260.
- Schwindt, G., & Rezmovitz, J. (2017). Essential tremor. *CMAJ*, 189(44), E1364.
- S. Sharifi, A. J. Nederveen, J. Booij, and A. F. Van Rootselaar, “Neuroimaging essentials in essential tremor: A systematic review,” *NeuroImage: Clinical*, vol. 5. Elsevier Inc., pp. 217–231, 01-Jan- 2014.
- Stoodley, C. J., Valera, E. M., & Schmahmann, J. D. (2012). Functional topography of the cerebellum for motor and cognitive tasks: An fMRI study. *NeuroImage*, 59(2), 1560–1570.
- P. L. Strick, R. P. Dum, and J. A. Fiez, “Cerebellum and nonmotor function,” *Annual Review of Neuroscience*, vol. 32. Annual Reviews, pp. 413–434, 25-Jun- 2009.
- Sultan, F., Hamodeh, S., & Baizer, J. S. (2010). The human dentate nucleus: A complex shape untangled. *Neuroscience*, 167(4), 965–968.
- Tiemeier, H., Lenroot, R. K., Greenstein, D. K., Tran, L., Pierson, R., & Giedd, J. N. (2010). Cerebellum development during childhood and adolescence: A longitudinal morphometric MRI study. *NeuroImage*, 49(1), 63–70.
- Tong, T., Gao, Q., Guerrero, R., Ledig, C., Chen, L., & Rueckert, D. (2016). A novel grading biomarker for the prediction of conversion from mild cognitive impairment to Alzheimer's disease. *IEEE Transactions on Biomedical Engineering*, 9294(c), 1–1.
- Tustison, N. J., Avants, B. B., Cook, P. A., Zheng, Y., Egan, A., Yushkevich, P. A., & Gee, J. C. (2010). N4ITK: Improved N3 bias correction. *IEEE Transactions on Medical Imaging*, 29(6), 1310–1320.
- Wang, H., Chen, H., Wu, J., Tao, L., Pang, Y., Gu, M., ... Fang, W. (2018). Altered resting-state voxel-level whole-brain functional connectivity in depressed Parkinson's disease. *Parkinsonism & Related Disorders*, 50, 74–80.
- Yang, Z., Ye, C., Bogovic, J. A., Carass, A., Jodynak, B. M., Ying, S. H., & Prince, J. L. (2016). Automated cerebellar lobule segmentation with application to cerebellar structural analysis in cerebellar disease. *NeuroImage*, 127, 435–444.

SUPPORTING INFORMATION

Additional supporting information may be found online in the Supporting Information section at the end of this article.

How to cite this article: Hett K, Lyu I, Trujillo P, et al. Anatomical texture patterns identify cerebellar distinctions between essential tremor and Parkinson's disease. *Hum Brain Mapp*. 2021;42:2322–2331. <https://doi.org/10.1002/hbm.25331>